Advances in Nano Research, *Vol. 10, No. 5 (2021) 437-448*
DOI: https://doi.org/10.12989/anr.2021.10.5.437

The investigation of Magnetohydrodynamic nanofluid flow with Arrhenius energy activation

Humaira Sharif[1], Mohamed A. Khadimallah[2,3], Muhammad Nawaz Naeem[1], Muzamal Hussain[1*], S.R. Mahmoud[4], K.S.Al-Basyouni[5] and Abdelouahed Tounsi[6,7]

[1]*Department of Mathematics, Govt. College University Faisalabad, 38000, Faisalabad, Pakistan*
[2]*Prince Sattam Bin Abdulaziz University, College of Engineering, Civil Engineering Department, BP 655, Al-Kharj, 16273, Saudi Arabia*
[3]*Laboratory of Systems and Applied Mechanics, Polytechnic School of Tunisia, University of Carthage, Tunis, Tunisia*
[4]*GRC Department, Faculty of Applied studies, King Abdulaziz University, Jeddah, Saudi Arabia*
[5]*Mathematics Department, Faculty of Science, King Abdulaziz University, Jeddah, Saudi Arabia*
[6]*YFL (Yonsei Frontier Lab), Yonsei University, Seoul, Korea*
[7]*Department of Civil and Environmental Engineering, King Fahd University of Petroleum & Minerals, 31261 Dhahran, Eastern Province, Saudi Arabia*

(*Received October 19, 2020, Revised January 1, 2021, Accepted January 11, 2021*)

Abstract. In this article, an analytically and numerically 3D nanoliquid flow by a porous rotatable disk is presented in the presence of gyrotactic microorganisms. The mathematical model in the form of partial differential system is transmuted into dimensionless form by utilizing the appropriate transformation. The homotopy analysis approach is applied to attain the analytic solution of the problem. The effect of promising parameters on velocity distribution, temperature profile, nanoparticles volume fraction and motile microorganism distribution field are evaluated through graphs and in tabular form. The existence of Brownian motion and thermophoresis impacts are more proficient for heat transfer enhancement. Further the unique features like heat absorption/generation and energy activation are also examined for the present flow problem. The obtained results are compared with the earliear investigation to check the accuracy of present model.

Keywords: nanoparticles; rotating disk; Arrhenius energy activation; bio-convection; MHD; HAM

1. Introduction

Rotating disk bio-reactors are important for various chemical engineering and medical phenomenons such as swirl-assisted pumping, chromatography, transfer of oxygen and purification. The advancement in the field of bio-engineering embraced new phenomenon such as bio-convection of microorganisms (oxy-tactic, photo-tactic, gyrotactic, magneto-tactic etc). Nanofluids show great thermal ability for example nano-particles are mixed with base fluids that show large number of applications in technological processes. Now a days, the investigators are engaged in investigating the flow of fluid across a rotatable disk. Because of its unique applications in various areas of science like engineering branches and aeronautical science such as electrical appliances, processes of crystal growth, computer storage equipments, rotatable machinery, medical instruments, vacuum cleaner instruments, gas turbine rotors and others (Hu *et al*. 2015, Hu 2016, Wang *et al*. 2017).

Firstly, Von Karman (1921) investigated the innovative work on flow of fluid through a rotatable plane. He applied momentum- integral procedure to investigate the resulting outcomes analytically. Impact of Suction/ injection in Von Karman problem was analyzed by Ackroyd (1978) and he found series solution comprising decaying parameters exponentially. Further, Miclavcic and Wang (2004) made an extension of the Von Karman problem where surface of disk accepts slip conditions. After the Von Karman's work, many researchers examined the interesting features of rotatable disk by using different conditions. Aziz *et al*. (2018) considered the MHD stream of nanoliquids by pivoting plate which revolves around its on axis with fractional slip. Gholinia *et al*. (2019) analyzed the Powel-Eyring nano liquid flow through a rotatable disk. They noted that temperature distribution boosted with the increase of thermophoresis parameter and shows decline behaviour with an increase of Prandtl number. Ahmed *et al*. (2019) analyzed the thin film flow of Maxwell nanoliquid through a rotatable disk in the presence of a non-linear thermal radiation and magnetic parameter. They observed that film thickness shows downturn with enhancing values of the magnetic parameter.

A few more fascinating work in this direction can be seen in Hafeez *et al*. (2020), Zaho *et al*. (2020), Shah *et al*. (2019). A nanofluid is a fluid that consist of petty gravimetric analysis of nanometer scale i.e., less than 100 nm particles is known as nanoparticles. These nanoparticles are commonly made from oxides, carbides, carbon nanotubes and metals. Different base fluids such as glycol, ethylene, oil and water are extremely utilized in different

*Corresponding author, Ph.D., (Research scholar)
E-mail: muzamal45@gmail.com
muzamalhussain@gcuf.edu.pk

ISSN: 2287-237X (Print), 2287-2388 (Online)

industrial procedures for heat transfer. Outstanding heat transport capacity is basic need in various engineering and industrial procedures such as glass fiber, production of papers, power generation and chemical procedures etc. Anyhow, the low conductivity of such type of base liquids is not plentiful to obtain the maximum thermal conductivity. The nanoparticles are used to increase the straight heat transport in various nuclear reactors, transportation, biomedicine, food and industrial fields etc. In different procedures, nanoliquids with greater thermophysical properties are utilized as potential heat transport liquids to obtain the excellent performance of heat transport. Moreover, nanofluids are utilized in engine cooling, cooling in machines, chillers, enhancement in heat transfer capacity of domestic refrigerators and freezers, heat transfer appliances, electronics cooling, space etc. Wang *et al*. (2019) studied the novel multi-segment mirror hybrid solar concentration photovoltaic/thermal (CPV/T) system using the spectral beam splitting technology and its composition, working principle and structural design method are introduced in this paper. The Needle optimization method is employed to design the spectral beam splitter for the CPV/T system. The Monte Carlo Ray Tracing method is used to simulate the solar concentrating process. Choi (1995) was the first who introduced a unique type of fluid called nanofluid during his research work on new cooling technologies and coolants. Analytic model for convective transfer in nanoliquids was analyzed by Buongiorno (2006). In this investigation he observed that there are seven feasible mechanisms that relate nanofluids convection by movement of nanoparticles in the base liquid. These include size of nanoparticle, Effect of magnus, inertia, Brownian motion, particle agglomeration, thermophoresis and volumetric fraction of nanoparticle. In all these above mechanisms thermophoresis and Brownian motion are very essential. The thermophoresis works across temperature gradient, in order to make, the particles movement from area of higher temperature to the area of lower temperature. And, due to Brownian motion particles tend to move from area of higher concentration to area of lower concentration. Yu *et al*. (2020) investigated the NO_x degradation performance of nano-TiO_2 as a coating material for the road environment was evaluated in this research. The nano-TiO_2 coating materials for both road surface and roadside were prepared by using anatase nano-TiO_2, activated carbon powder, silane coupling agent and deionized water. The impact of varying amounts of coating material and silane coupling agent were evaluated. Rashidi *et al*. (2013) have deliberated that the flow of nanofluid through a rotatable permeable disk with entropy generation and magnetic parameter. Sheikholeslami *et al*. (2014) noted transfer of heat and boundary layer flow of nanofluid by a rotatable disk. Guo *et al*. (2020) designed a high-efficiency sensing system for α-synuclein (α-Syn) oligomers was designed based on a novel one dimensional (1D)/2D structural nanohybrid (denoted as CoMnZIF@ CNF) of CoMn-based zeolitic imidazolate framework nanosheets (CoMnZIF NSs) vertically grown around carbon nanofibers (CNFs). CNFs were prepared by calcining electrospun polyacrylonitrile under Ar/H_2 atmosphere and used as the template for CoMnZIF synthesis. Sheikholeslami *et al*. (2020a) studies the swirl generator and four-lobed pipe in a solar collector to achieve higher performance not only in view of cooling rate but also available energy. In outputs, components of irreversibility were illustrated for different values of revolution (N), pumping power (Re (Reynolds number)) and width of tapes (D*(diameter ratio)). Four functions were scrutinized namely, Xd (exergy loss), S gen, th (thermal irreversibility), S gen, f (frictional irreversi-bility), Φ s (Augmented irreversibility). Turkyilmazoglu (2014) discussed Magnetohydrodynamic nanofluid flow and transfer of heat through a rotatable disk. Khan *et al*. (2020) analyzed the Magneto rotatable flow of hybrid nanolfluid along entropy generation. Li *et al*. (2002) explored the higher requirements for the performance of cement-based materials and the call for energy conservation and environmental protection, a wave of research on new materials has set off, and various high-performance concrete and more environmentally friendly geopolymers. With a view to solving the defects of energy consumption, environmental protection and low toughness of traditional cement-based materials. Sheikholeslami *et al*. (2013) investigated the analytical approach of MHD nanoliquid outflow in a semi-permeable channel. They observed that thickness of velocity boundary layer decline by increasing the value of Reynold number and it shows increase in Hartmann number to attain maximum value. Ma *et al*. (2019) examined the numerical investigation of MHD nanoliquid natural convection in a U-shape enclosure. Shah *et al*. (2019) analyzed the effect of non-linear thermal radiations on MHD nanoliquid thin film outflow through a horizontal rotatable disk. Yan *et al*. (2020) studied the polypyrrole-modified $NaTi_2$ $(PO_4)_3$ ($NaTi_2$ $(PO_4)_3$ @ PPy) nanocomposite for sodium energy storage via the sol-gel approach and the self-assembly procedure. The physical and electrochemical performances for the resulted $NaTi_2$ $(PO_4)_3$@ PPy have been characterized in this research. Benefiting from the conductive polypyrrole coating, the $NaTi_2$ $(PO_4)_3$@ PPy displays outstanding sodium storage property with the specific capacity of 95.9 mAh g-1 at 20 C after 400 cycles. Gabriela and Angel (2020) discussed the entropy generation of hybrid nanoliquid and nanoliquid outflow in thermal structure. Subhani and Nadeem (2019) examined the numerical approach of micropolar hybrid nanoliquid. Few recent investigations related to nanofluids may be viewed in Ghalandari *et al*. (2019), Tlili *et al*. (2019), Nasiri *et al*. (2019).

Sheikholeslami *et al*. (2020b) investigated a clean energy storage unit to decrease the energy consumption through the building. To increase the space between the passing air and the Phase change material (PCM), instead of a smooth channel, a sinusoidal channel has been considered for the airway passage. Furthermore, porous media and nanoparticles have been applied in this unit for the purpose of enhancing heat transfer. Considering previous research works, the simultaneous use of these three methods for augmenting the performance has not been scrutinized so far. In this study, three mechanisms for augmenting heat transfer and the interaction of these methods to augment the performance of the system have been evaluated. Based on

comparison with experimental data, outputs are very excellent fit with maximum 9.3% deviation. Magneto-hydrodynamics is also known as hydromagnetics which deals with the behavior of electrical conductive fluids and magnetic properties like liquid metals, electrolytes, salt water and plasma. The investigation of magneto-hydrodynamic flow has a large number of applications in fields of engineering and technology. Therefore, numerous investigators represented their research work in Magnetohydrodynamics flows. Sheikholeslami and Farshad (2020) analyzed the nanoparticle turbulent transportation with install of helical tape within a solar system. Increasing radial turbulent fluctuation is main concept of utilizing the turbulator. So, install of such device generates secondary flow and produce thinner boundary layer. So, better mixing happens and consequently, cooling rate augments. With growth of secondary flow with rise of Re (Reynolds number), N (number of revolution) and NT (number of tapes). Zhao *et al*. (2019) accounted the Heat transport of the MHD nanofluid along permeable microtubes with electrokinetic impacts. Noghrehabadi *et al*. (2013) has analyzed the natural convection of nanoliquid through a vertical plate embedded in permeable media.

The process of bioconvection represented the instability and unstructured pattern that is produced by the microorganisms which swims on the upper part of a fluid that possess lesser density. Due to up swimming, these microorganisms included motile micro-organisms such as algae remains in the upper part of the liquid layer and creates unstable top heavy density stratification Pedley *et al*. (1988), Xun *et al*. (2017) tackled gravitactic micro-organisms used for bio-convection by a rotatable structure in nanoliquid. Saini and Sharma (2018) studied gravitactic microorganisms by using energy method. Chakraborty *et al*. (2018) analyzed the effects of external magnetic parameter on bio-convection flow which comprises of motile microorganism with convective conditions. Khan *et al*. (2020a, 2020b) talked about bioconvected nanofluid outflow between two stretching rotatable disks through Entropy generation. Waqas *et al*. (2019) provided bio-convection flow of second-grade nanoliquid (modified) with motile microorganisms along a stretchable surface. It is observed that gyrotactic microorganism distribution decreases with Prandtl number and Brownian movement parameter. Recently some researcher used different methods for nonlinear modeling (Eltaher *et al*. 2019, Ebrahimi *et al*. 2019, Safaei *et al*. 2019, Shahsavari *et al*. 2019, Benmansour *et al*. 2019).

After revisiting aforementioned papers, the intention here is to study the combined effects of energy activation and motile microorganism in MHD 3D flow of nanoparticles through a porous rotating disk with chemical reaction and convective conditions. Thermophoretic dispersal process and irregular movement occurs due to existence of nanoparticles. The governing mathematical model is tackled by homotopy analysis procedure. Further the characteristics of microorganisms, mass and heat transfer and related parameters present in the equations are examined through plots and tables.

2. Mathematical formulation

We consider three-dimensional MHD nanofluid flow with heat source/sink and immersed motile microorganisms over a porous rotatable disk. Arrhenius energy activation and effect of chemical reactions are also considered. Magnetic field acts in perpendicular direction. By using low Reynolds number assumption the impact of induced magnetic field is neglected. The disk is rotatable at $z = 0$ with constant angular velocity Ω. Impact of thermophoresis and Brownian dispersion is also present. Here (u, v, w) are the velocity components in the directions of rising (r, ϕ, z) respectively. For present flow problem the governing PDE's are

$$\frac{\partial u}{\partial r}+\frac{u}{r}+\frac{\partial w}{\partial z}=0 \tag{1}$$

$$u\frac{\partial u}{\partial r}-\frac{v^2}{r}+w\frac{\partial u}{\partial z}=\nu\left(\frac{\partial^2 u}{\partial r^2}+\frac{1}{r}\frac{\partial u}{\partial r}-\frac{u}{r^2}+\frac{\partial^2 u}{\partial z^2}\right)-\frac{\sigma' {B_0}^2}{\rho_f}u -\frac{\nu}{k^*}u+\frac{1}{\rho_f}\begin{bmatrix}\rho_f\beta(1-C_\infty)(T-T_\infty)-(\rho_p-\rho_f)(C-C_\infty)\\ -\gamma(\rho_m-\rho_f)(n-n_\infty)\end{bmatrix}g \tag{2}$$

$$u\frac{\partial v}{\partial r}+\frac{uv}{r}+w\frac{\partial v}{\partial z} =\nu\left(\frac{\partial^2 v}{\partial r^2}+\frac{1}{r}\frac{\partial v}{\partial r}-\frac{v}{r^2}+\frac{\partial^2 v}{\partial z^2}\right)-\frac{\sigma' {B_0}^2}{\rho_f}u-\frac{\nu}{k^*}v \tag{3}$$

$$u\frac{\partial w}{\partial r}+w\frac{\partial w}{\partial z}=\nu\left(\frac{\partial^2 w}{\partial r^2}+\frac{1}{r}\frac{\partial w}{\partial r}+\frac{\partial^2 w}{\partial z^2}\right) \tag{4}$$

$$u\frac{\partial T}{\partial r}+w\frac{\partial T}{\partial z}=\alpha_m{}^*\left(\frac{\partial^2 T}{\partial z^2}+\frac{\partial^2 T}{\partial r^2}+\frac{1}{r}\frac{\partial T}{\partial r}+\right) +\frac{Q_\circ}{(\rho c)_f}(T-T_\infty)+\frac{(\rho c)_p}{(\rho c)_f}\begin{pmatrix}D_B\left(\frac{\partial T}{\partial z}\frac{\partial C}{\partial z}+\frac{\partial T}{\partial r}\frac{\partial C}{\partial r}\right)\\ +\frac{D_T}{T_\infty}\left(\left(\frac{\partial T}{\partial z}\right)^2+\left(\frac{\partial T}{\partial r}\right)^2\right)\end{pmatrix} \tag{5}$$

$$u\frac{\partial C}{\partial r}+w\frac{\partial C}{\partial z}=D_B\left(\frac{\partial^2 C}{\partial z^2}+\frac{\partial^2 C}{\partial r^2}+\frac{1}{r}\frac{\partial C}{\partial r}\right) +\frac{D_T}{T_\infty}\left(\frac{\partial^2 T}{\partial z^2}+\frac{\partial^2 T}{\partial r^2}+\frac{1}{r}\frac{\partial T}{\partial r}\right)-{k_r}^2(C-C_\infty)\left(\frac{T}{T_\infty}\right)^n exp\left(-\frac{E_a}{\kappa T}\right) \tag{6}$$

$$u\frac{\partial n}{\partial r}+w\frac{\partial n}{\partial z}+\frac{bW_c}{C_\infty}\left[\frac{\partial}{\partial z}\left(n\frac{\partial C}{\partial z}\right)\right]={D_m}^*\left(\frac{\partial^2 n}{\partial z^2}+\frac{\partial^2 n}{\partial r^2}+\frac{1}{r}\frac{\partial n}{\partial r}\right) \tag{7}$$

The appropriate boundary conditions are

$$u=r\Omega,\quad w=0,\quad v=r\Omega,\quad -k_2\frac{\partial T}{\partial z}=h_2(T_w-T),\\ -k_3\frac{\partial C}{\partial z}=h_3(C_w-C),\quad -k_4\frac{\partial n}{\partial z}=h_4(n_w-n)\ \text{ at }\ z=0 \tag{8}$$

$$u\to 0,\ v\to 0,\ T\to T_\infty,\ C\to C_\infty,\ n\to n_\infty\ \text{ at }\ z\to\infty \tag{9}$$

where u, v and w denotes velocities in r, ϕ and z directions respectively, $\nu=\frac{\mu}{\rho_f}$ is kinematic viscosity, ρ_f is density of base fluid, μ is dynamic viscosity, k^* is porous surface, ${\alpha_m}^*=\frac{k}{(\rho c)_f}$ is thermal diffusivity, k is thermal conductivity, $(\rho c)_f$ is fluid heat capacity, $(\rho c)_p$ is effective heat capacity, T is liquid temperature, D_B the Brownian diffusivity factor, D_T the thermophoretic

coefficient, k_r the rate of reaction, C is concentration of nanoparticles, $Q_\circ$ is heat source/sink coefficient, $D_m{}^*$ is microorganism diffusion factor, W_c the maximum cell-swimming speed, κ is Boltzmann constant, C_w, C_∞, T_w, T_∞, n_w and n_∞ denotes the concentration, temperature and density of motile microorganisms which exist at and far away from the stretchable surface.

Following are similarity variables

$$u = r\Omega f'(\zeta), \quad w = -\sqrt{2\Omega\upsilon} f(\zeta), \quad v = r\Omega g(\zeta),$$
$$\zeta = \sqrt{\frac{2\Omega}{\upsilon}} z, \quad \theta(\zeta) = \frac{T - T_\infty}{T_w - T_\infty}, \quad \phi(\zeta) = \frac{C - C_\infty}{C_w - C_\infty}, \quad \chi(\zeta) = \frac{n - n_\infty}{n_w - n_\infty} \tag{10}$$

where ζ, $f(\zeta)$, $g(\zeta)$, $\theta(\zeta)$, $\phi(\zeta)$ and $\chi(\zeta)$ are similarity variable, dimensionless stream functions, dimensionless temperature, dimensionless concentration and dimension-less micro-organism function. Equation of continuity trivially holds, while by using Eq. (10) into Eqs. (2)-(9), we obtained

$$2f''' - \lambda f' + 2ff'' - f'^2 + g^2 - (Ha)^2 f' + \Lambda(\theta - Nr\phi - RbN) = 0 \tag{11}$$

$$2g'' - \lambda g + 2fg' - 2f'g - (Ha)^2 g = 0 \tag{12}$$

$$\frac{1}{Pr''''^2} \tag{13}$$

$$\frac{1}{sc}\phi'' + f\phi' + \frac{1}{sc}\frac{Nt}{Nb}\theta'' - \sigma(1+\omega\theta)^n exp\left(\frac{-E}{1+\omega\theta}\right)\phi = 0 \tag{14}$$

$$\chi'' + Lbf\chi' - Pe(\phi''(\chi + \delta) + \chi'\phi') = 0 \tag{15}$$

Associated boundary conditions are

$$f(0) = 0, \quad f'(0) = 1, \quad g(0) = 1, \quad \theta'(0) = -B_{i1}(1 - \theta(0)), \quad \phi'(0) = -B_{i2}(1 - \phi(0)), \quad \chi'(0) = -B_{i3}(1 - \chi(0)) \tag{16}$$

$$f'(\infty) \to 0, \quad g(\infty) \to 0, \quad \theta(\infty) \to 0, \quad \phi(\infty) \to 0, \quad \chi(\infty) \to 0 \tag{17}$$

where $(Ha)^2 = \frac{\sigma' B_\circ{}^2}{\Omega\rho_f}$ is Hartman number, $Pr = \frac{\upsilon}{\alpha_m{}^*}$ is Prandtl number, $\lambda = \frac{\upsilon_f}{\Omega k^*}$ is porosity coefficient, $Nb = \frac{D_B(\rho c)_p(C_w - C_\infty)}{(\rho c)_f \upsilon}$ is Brownian movement coefficient, $Nt = \frac{(\rho c)_p D_T(T_w - T_\infty)}{(\rho c)_f \nu T_\infty}$ is Thermophoresis coefficient, $\tau = \frac{Q_\circ}{2\Omega(\rho c)_f}$ is heat sink/source coefficient, $Sc = \frac{\nu}{D_B}$ is Schmidt number, $Lb = \frac{\alpha}{D_m{}^*}$ is bio-convected Lewis number, $Pe = \frac{bW_c}{\nu}$ is bio-convected Peclet number, $\sigma = \frac{kr^2}{\Omega}$ is chemical reaction coefficient, $E = \frac{E_a}{kT_\infty}$ is dimensionless energy activation, $\delta = \frac{T_w - T_\infty}{T_\infty}$, $B_{i1} = \frac{h_2}{k_2}\sqrt{\frac{\upsilon}{2\Omega}}$ is Biot number, $\lambda = \frac{g\beta(1-C_\infty)(T_w - T_\infty)}{r\Omega^2}$ is mix convection coefficient, $Nr = \frac{(\rho_p - \rho_f)(C_w - C_\infty)}{\beta(1-C_\infty)(T_w - T_\infty)}$ is Buoyancy ratio coefficient, $R_b = \frac{\gamma(\rho_m - \rho_f)(n_w - n_\infty)}{\beta(1-C_\infty)(T_w - T_\infty)}$ is Bioconvection Rayleigh number.

The dimensionless forms of shear stress of wall, local Nusselt number, local Sherwood and motile micro-organisms are

$$\sqrt{Re_r}C_f = -f''(0), \quad \sqrt{Re_r}C_g = -g'(0), \quad \frac{Nu}{\sqrt{Re_r}} = -\theta'(0), \quad \frac{Sh}{\sqrt{Re_r}} = -\phi'(0), \quad \frac{N_n}{\sqrt{Re_r}} = -\chi'(0) \tag{18}$$

where $Re_r = \frac{2r(r\Omega)}{\nu}$ denotes the Reynolds number.

3. Problem Solution

In order to find the solutions of Eqs. (11)-(15) with boundary conditions (16)-(17), we impliment Homotopy analysis method. HAM methodology is useful for the solution of BVPs as it does not consider small or large parameters in case of perturbation methods. This scheme gives an easy way to confirm the solution convergence. Furthermore, it provides an easy method for the selection of base and auxiliary parameters. In this procedure, the auxiliary parameter $\hbar$ is commonly used to support the problem convergence. The appropriate initial guesses and linear operators are presented in the form

$$f_0(\eta) = 1 - e^{-\eta}, \quad g_0(\eta) = e^{-\eta}, \quad \theta_0(\eta) = \frac{B_{i1}}{1 + B_{i1}}e^{-\eta}, \quad \phi_0(\eta) = \frac{B_{i2}}{1 + B_{i2}}e^{-\eta}, \quad \chi_0(\eta) = \frac{B_{i3}}{1 + B_{i3}}e^{-\eta} \tag{19}$$

$$L_f = f''' - f', \quad L_g = g'' - g, \quad L_\theta = \theta'' - \theta, \quad L_\phi = \phi'' - \phi, \quad L_\chi = \chi'' - \chi \tag{20}$$

As discussed in the above differential operators, contents are presented below

$$\begin{aligned} &L_f[A_1{}^* + A_2{}^* e^{\eta} + A_3{}^* e^{-\eta}] = 0, \\ &L_g[A_4{}^* e^{\eta} + A_5{}^* e^{-\eta}] = 0, \\ &L_\theta[A_6{}^* e^{\eta} + A_7{}^* e^{-\eta}] = 0, \\ &L_\phi[A_8{}^* e^{\eta} + A_9{}^* e^{-\eta}] = 0, \\ &L_\chi[A_{10}{}^* e^{\eta} + A_{11}{}^* e^{-\eta}] = 0 \end{aligned} \tag{21}$$

Here $A_i{}^*$ $(i = 1, 2, 3, \ldots\ldots, 11)$ indicates the arbitrary constants.

4. Convergence analysis

By using the homotopy analysis method when the series solutions are evaluated for the velocity, temperature, concentration and microorganism functions, the auxiliary parameters are $\hbar_f$, $\hbar_\theta$, $\hbar_\phi$ and $\hbar_\chi$. These major parameters are responsible for the solution convergence. So, related $\hbar$ -curves are represented in Fig. 2. For such problems the values of appropriate convergence are $-1.1 \leq \hbar_f \leq 0.1$, $-1.1 \leq \hbar_g \leq 0.4$, $-1.6 \leq \hbar_\theta \leq 0.2$, $-1.5 \leq \hbar_\phi \leq 0.1$, $-1.6 \leq \hbar_\chi \leq 1.0$.

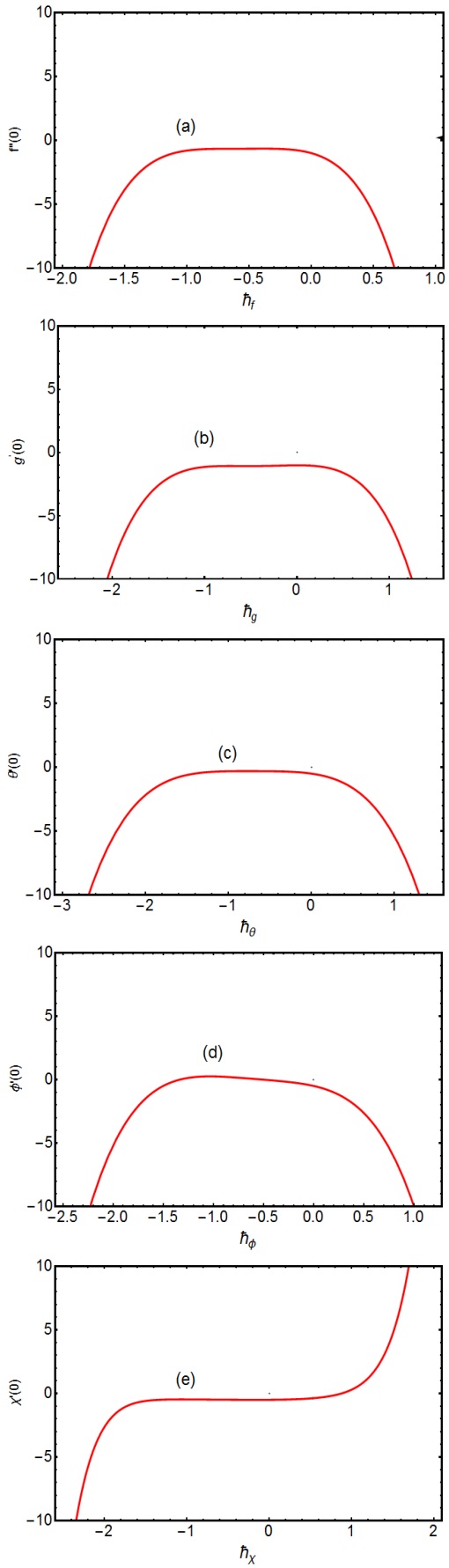

Fig. 1 Visualize the $\hbar$–curves of $f''(0)$, $g'(0)$, $\theta'(0)$, $\phi'(0)$ and $\chi'(0)$

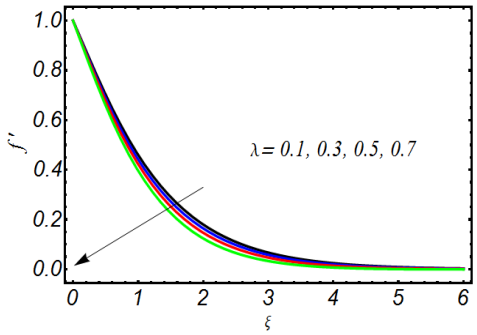

Fig. 2 Visualize the influence of λ on f'

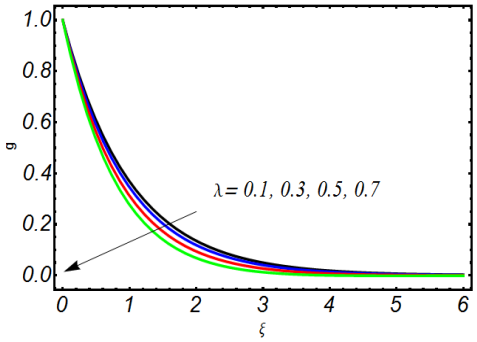

Fig. 3 Visualize the influence of λ on g

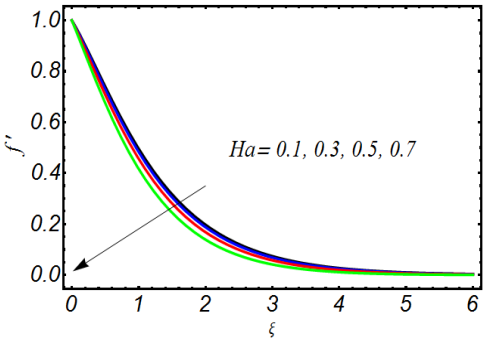

Fig. 4 Visualize the influence of Ha on f'

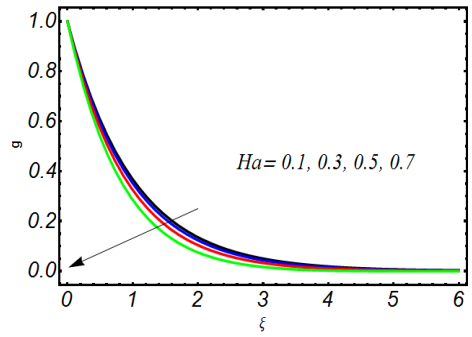

Fig. 5 Visualize the influence of Ha on g

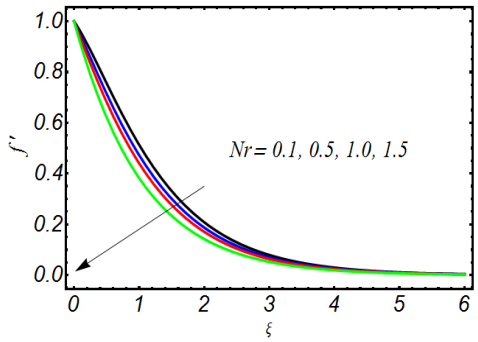

Fig. 6 Visualize the influence of Nr on f'

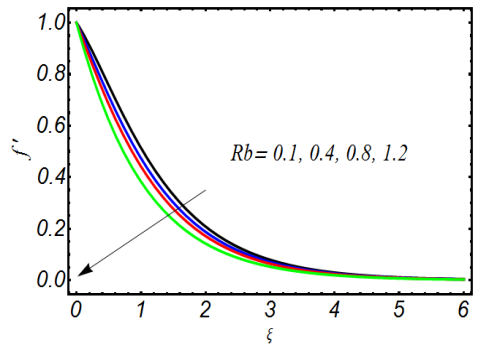

Fig. 7 Visualize the influence of Rb on f'

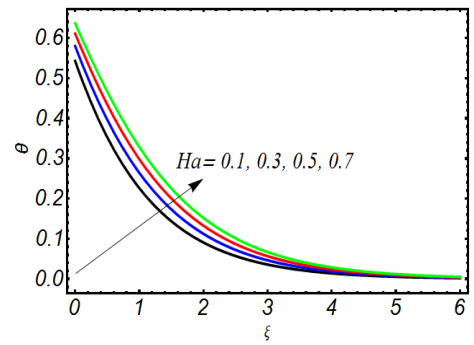

Fig. 8 Visualize the influence of Ha on θ

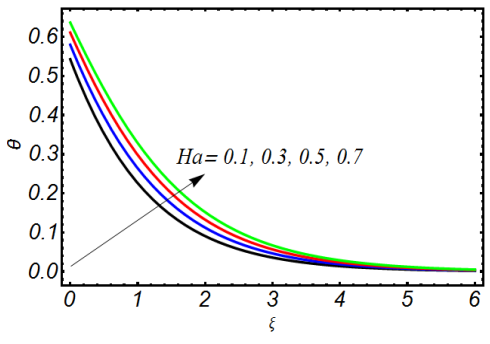

Fig. 9 Visualize the influence of τ on θ

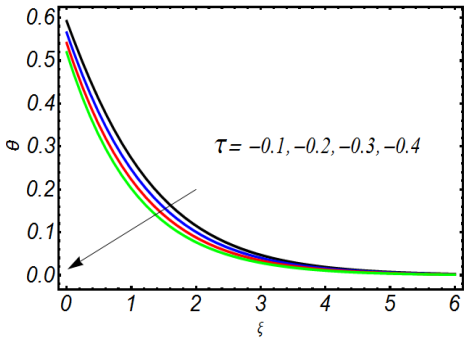

Fig. 10 Visualize the influence of τ on θ

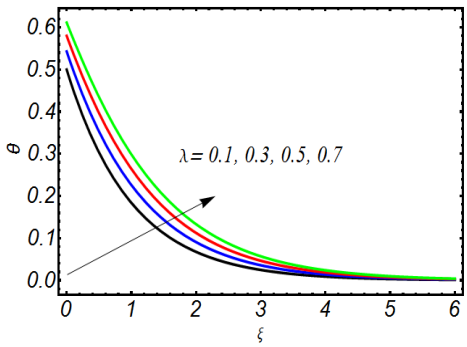

Fig. 11 Visualize the influence of λ on θ

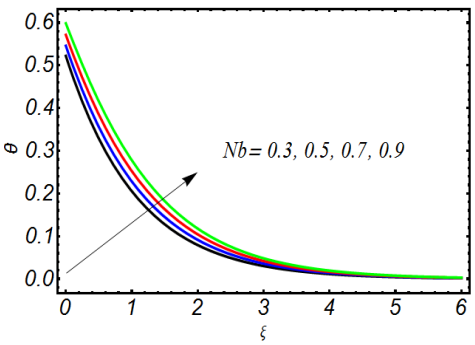

Fig. 12 Visualize the influence of Nb on θ

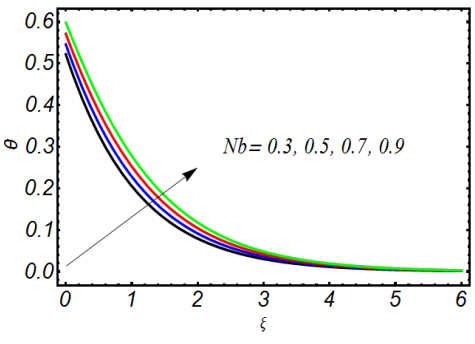

Fig. 13 Visualize the influence of Nt on θ

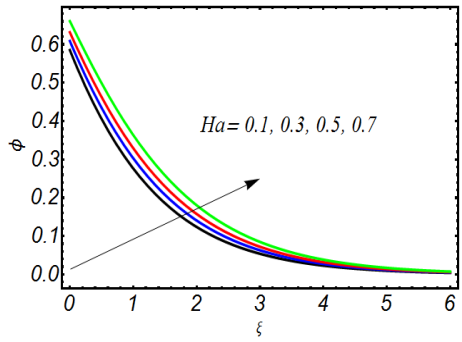

Fig. 14 Visualize the influence of Ha on ϕ

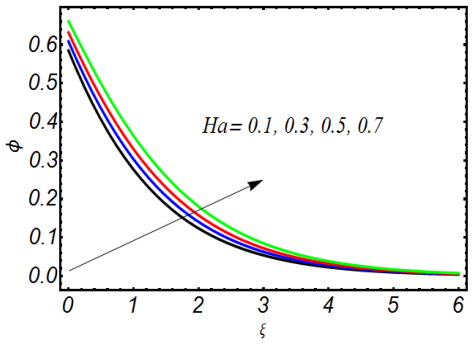

Fig. 15 Visualize the influence of E on ϕ

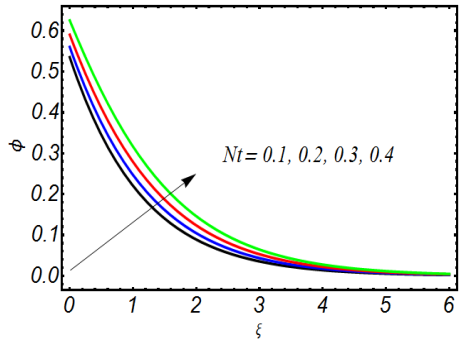

Fig. 16 Visualize the influence of Nt on ϕ

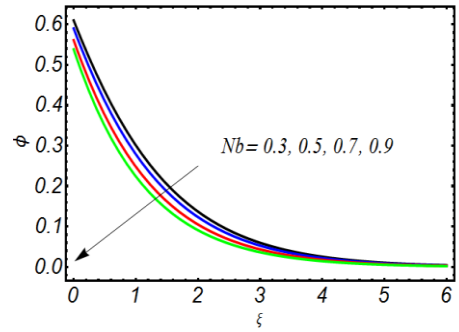

Fig. 17 Visualize the influence of Nb on ϕ

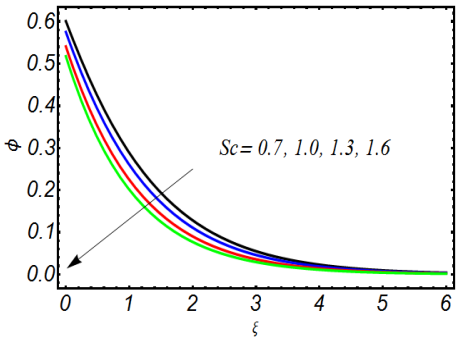

Fig. 18 Visualize the influence of Sc on ϕ

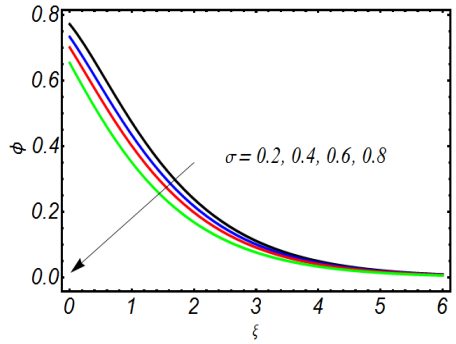

Fig. 19 Visualize the influence of σ on ϕ

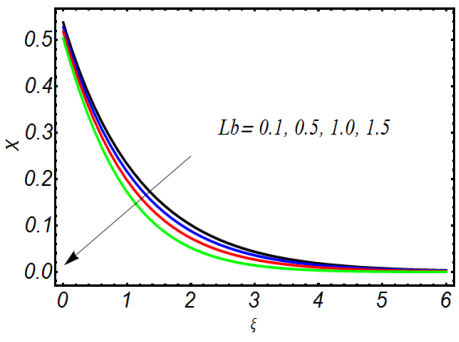

Fig. 20 Visualize the influence of Lb on ϕ

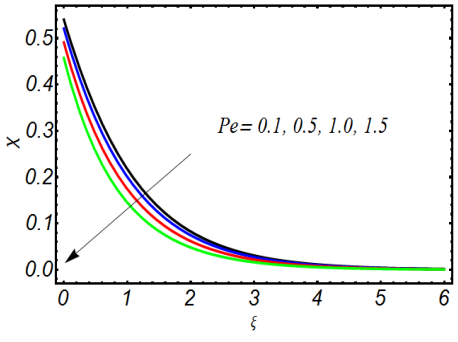

Fig. 21 Visualize the influence of Pe on ϕ

Table 1 Convergence of present results with Sharma and Gupta (2017)

Order of approximation	$-f''(0)$		$-\theta'(0)$		$-\varphi'(0)$	
	Sharma and Gupta (2017)	Present	Sharma and Gupta (2017)	Present	Sharma and Gupta (2017)	Present
1	2.57333	2.56547	0.888235	0.888139	2.03667	2.03645
3	2.53480	2.52883	0.888136	0.888112	2.04223	2.04220
5	2.53266	2.53211	0.887391	0.887299	2.04361	2.04351
10	2.53252	2.53209	0.887262	0.887246	2.04386	2.04371
15	2.53252	2.53208	0.887184	0.887099	2.04402	2.04399
20	2.53252	2.53208	0.887102	0.88700	2.04022	2.04019

Table 2 Numerical values of $C_{fx}(0)$for different values of parameters. When $Pr = Sc = B_{i2} = n = Lb = 1, Nt = \lambda = 0.2,\ Nb = Ha = Pe = 0.3,\ B_{i1} = B_{i3} = 0.4,\ Nr = E = \delta = \Lambda = 0.1,\ \tau = -0.1,\ \omega = \sigma = 0.01$

Ha	λ	Nr	Rb	$-f''(0)$	$-g'(0)$
0.3				0.7511	1.1134
0.5	0.2	0.1	0.1	0.7972	1.1458
1.0				0.9912	1.2904
	0.3			0.7801	1.1337
	0.5			0.8361	1.1737
	0.7			0.8892	1.2128
		0.3		0.7557	1.1123
		0.4		0.7576	1.1118
		0.5		0.7603	1.1113
			0.3	0.7529	1.1130
			0.5	0.7547	1.1127
			0.7	0.7567	1.1122

Table 3 Numerical values of $-\theta'(0)$ for different values of parameters. When $Pr = Sc = 2,\ Nt = \lambda = 0.2,\ Nb = Ha = 0.3,\ B_{i1} = B_{i3} = 0.4,\ B_{i2} = n = Lb = 1, \tau = -0.1,\ E = \delta = \Lambda = 0.1,\ \sigma = \omega = 0.01$

Ha	λ	Nt	Nb	Sc	Pr	τ	$-\theta'(0)$
0.3							0.2658
0.5	0.2	0.2	0.3	2.0	2.0	-0.1	0.2654
0.7							0.2642
	0.4						0.2649
	0.6						0.2642
	0.8						0.2636
		0.3					0.2612
		0.5					0.2539
		0.7					0.2490
			0.4				0.2608
			0.6				0.2514
			0.8				0.2417
				3.0			0.2632
				4.0			0.2622
				5.0			0.2616
					3.0		0.2801
					4.0		0.2883
					5.0		0.2939
						0.0	0.2541
						-0.05	0.2601
						-0.1	0.2658

Table 4 Numerical values of $-\phi'(0)$ for different values of parameters. When $Pr = Sc = 2.0$, $Nt = Ha = \lambda = 0.2$, $Nb = 0.3$, $B_{i2} = n = Lb = 1$, $B_{i1} = B_{i3} = 0.4$, $\tau = -0.1$, $\omega = \sigma = 0.01$, $Nr = Rb = \delta = \Lambda = 0.1$, $E = 1.0$

Ha	λ	Nt	Nb	Sc	Pr	$-\phi'(0)$
0.2						0.4016
0.3	0.2	0.2	0.3	2.0	2.0	0.4003
0.5						0.3960
	0.3					0.3989
	0.5					0.3937
	0.7					0.3885
		0.2				0.4016
		0.3				0.3748
		0.4				0.3487
			0.1			0.2674
			0.5			0.4272
			0.7			0.4410
				2.0		0.4016
				2.5		0.4423
				3.0		0.4687
					1.5	0.4057
					2.5	0.3986
					3.0	0.3962

Table 5 Numerical values of $-\chi'(0)$ for different values of parameters. When $Pr = Sc = 2.0$, $Nt = Ha = \lambda = 0.2$, $Nb = 0.3$, $B_{i1} = B_{i3} = 0.4$, $B_{i2} = n = Lb = Pe = Nr = 1.0$, $\omega = \delta = \sigma = 0.01$, $E = \Lambda = 0.1$, $Rb = 0.8$

Lb	Pe	Nr	Rb	$-\chi'(0)$
1.0				0.2885
1.1	1.0	1.0	1.0	0.2913
1.2				0.2925
	0.0			0.2406
	1.0			0.2885
	1.1			0.2912
		0.1		0.2875
		0.4		0.2877
		0.8		0.2879
			0.1	0.2875
			0.4	0.2863
			0.8	0.2861

5. Results and discussion

The major purpose of this section is to elaborate the various interesting parameters on velocities, temperature, concentration and microorganism profiles. The results are compared with the earliear investigations of Sharma and Gupta (2017).

Figs. 2 and 3 display the influence of porosity parameter on velocity profiles. It is observed that for large values of porosity parameter λ, the velocities f' and g adopt decreasing trend. Physically, porosity parameter depends on the porous material permeability. In case of large porosity parameter the porous material permeability is weaker. So, the output of this weaker porous material permeability shows the decreasing behavior of f' and g. Figs. 4 and 5 interpret that velocities f' and g decrease for large values of Hartman number Ha. Here Hartman number $Ha = 0$ denotes the flow case of hydrodynamic and $Ha \neq 0$ represents the circumstance of hydromagnetic flow. The influence of buoyancy ratio parameter Nr and bioconvection Rayleigh number Rb on velocity distribution f' is visualized in Figs. 6 and 7. It is noticed that an increment of Nr and Rb, a decrement in velocity distribution is observed. Greater buoyancy ratio parameter is liable for higher buoyancy force because of concentration and that is responsible for decrement in velocity distribution.

Fig. 8 demonstrates the affect of Hartman number on temperature profile θ. It is noted that higher values of Ha, the Lorentz force increases which enhance the resistance of fluid flow as a result temperature enhance. The impact of heat source/sink parameter on temperature dispersion is delineated in Figs. 9 and 10. Here $\delta > 0$ shows heat source and $\delta < 0$ for heat sink. For large values of δ, thermal layer and temperature θ increases. The impact of porosity parameter λ on temperature dispersion is expressed in Fig. 11. It is noted that temperature profile θ increases rapidly when λ rises. Physically, the lesser porous material permeability produces corresponding to higher λ. The lesser porous material permeability corresponds to high temperature. Fig. 12 represents variety in temperature profile for distinct values of Brownian movement Nb. Here

temperature profile θ is boosted directly with Nb. Physically, by increasing Brownian motion Nb the sporadic movement of nanoparticles enhances and the promoted diffusion raises the temperature. As a result, kinetic energy is changed into heat energy which shows an increment in related layer thickness and temperature distribution θ. Influence of thermophoresis parameter Nt on temperature distribution is represented in Fig. 13. By increasing values of Nt resulted higher temperature field and enhanced thermal layer thickness.

Fig. 14 indicated the effect of Hartman parameter Ha on concentration field. By enhancing Ha, both the concentration layer and concentration profile are increased. Fig. 15 explains the effect of dimensionless energy activation paramerer E on concentration profile. The advancement in energy activation with modified Arrhenius work, inevitably develops generative synthetic reaction to increase concentration profile. Fig. 16 explains that how thermophoresis parameter Nt influence the concentration distribution. For large values of Nt, the thickness of related layer at the boundary for concentration profile is boosted. The impact of Brownian motion coefficient Nb on concentration field is portrayed in Fig. 17. It is observed that fragile concentration field is generated by utilizing greater Brownian motion Nb. From Fig. 18, we noted that for higher values of Schmidt parameter Sc, the concentration profile declines. Physically, the Schmidt parameter Sc is inversely proportional to Brownian diffusivity. Enhancing Schmidt parameter yields a lesser Brownian diffusivity. This lesser Brownian diffusivity leads to decline concentration profile. Fig. 19 shows the impact of chemical reaction coefficient σ on concentration field. It is noted that increasing this coefficient, concentration profile and thickness of related layer at boundary decreases.

Fig. 20 represents the influence of bio-convection Lewis number Lb on microorganism density profile. A rapid declining behavior is observed for microorganism density profile for higher values of Lb. This is because the bio-convection Lewis number Lb is opposite to the diffusion procedure. The impact of Peclet number Pe on motile density profile is shown in Fig. 21. For large values of Pe, density profile is reverted. The maximal speed of swimming cell is increased with enhancement in Pe. Due to maximal speed of swimming cell the density profile is reduced. To report the values of $g'(0)$ and $f''(0)$ in response to different values of λ, Ha, Nr and Rb, Table 2 is constructed. For large values of Nr and Rb the numerical values of $f''(0)$ becomes larger and $g'(0)$ becomes smaller. Table 3 shows the numerical values of local Nusselt number for distinct values of $Ha, \lambda, Nt, Nb, Sc,$ Pr and τ. We observed that local Nusselt number decays for large values of Ha, λ, Nt and Nb. Table 4 indicated the numerical values of local Sherwood number for various values of Ha, λ, Nt, Nb, Sc and Pr. It is noted that for higher values of Ha, λ and Nt, Sherwood number decreases. Table 5 shows the local motile microorganism for different values of Lb, Pe, Nr and Rb. Local motile microorganism number is increased rapidly with increasing values of Lb, Pe and Nr.

6. Conclusions

In this study, the characteristics of motile microorganism distribution and MHD three dimensional viscous nanofluid flow through a porous rotatable disk with chemical reaction, Arrhenius energy activation and heat generation/absorption have been exaimened. Homotopy analysis procedure is implemented to derive the analytic results of physical quantities are evaluated parametrically. For increasing the Hartman number Ha, the velocities f' and g decreases while the concentration, temperature and microorganism increases. For large values of Porosity parameter λ, the velocities f' and g shows decreasing behavior. For higher values of buoyancy ratio coefficient$Nr$and bioconvection Rayleigh number Rb, velocity distribution f' decline. In the presence of thermophoresis constraint shows similar behavior for both temperature and concentration profile. Concentration distribution shows decline behavior for large values of σ and Sc. By increasing the values of bio-convected peclet number Pe and bio-convected Lewis number Lb, the motile microorganism is decline rapidly. The reported observations can be efficiently used in the improvement of transfer of heat devices as well as microbial fuel cells.

Declaration of Conflicting Interests

The author(s) declared no potential conflicts of interest with respect to the research, authorship, and/or publication of this article.

Acknowledgement

This project was supported by the Deanship of Scientific Research at Prince Sattam Bin Abdulaziz University under the research project No 16794/01/2020.

ORCID ID

Muzammal Hussain
http://orcid.org/0000-0002-6226-359X

References

Ackroyd, J.A.D. (1978), "On the steady flow produced by a rotating disc with either surface suction or injection", *J. Eng. Math*., **12**(3), 207-220. https://doi.org/10.1007/BF00036459.

Ahmed, J., Khan, M. and Ahmad, L. (2019), "Transient thin film flow of nonlinear radiative Maxwell nanofluid over a rotating disk", *Phys. Lett. A*, **383**(12), 1300-1305. https://doi.org/10.1016/j.physleta.2019.01.024.

Aziz, A., Alsaedi, A., Muhammad, T. and Hayat, T. (2018), "Numerical study for heat generation/absorption in flow of nanofluid by a rotating disk", *Results Physi*., **8**, 785-792. https://doi.org/10.1016/j.rinp.2018.01.009.

Benmansour, D.L., Kaci, A., Bousahla, A.A., Heireche, H., Tounsi, A., Alwabli, A.S., Alhebshi, A.M., Al-ghmady, K., Mahmoud,

S.R. (2019), "The nano scale bending and dynamic properties of isolated protein microtubules based on modified strain gradient theory", *Adv. Nano Res., Int. J.*, **7**(6), 443-457. https://doi.org/10.12989/anr.2019.7.6.443.

Buongiorno, J. (2006), "Convective transport in nanofluids", *ASME. J. Heat Transfer.*, **128**(3), 240-250. https://doi.org/10.1115/1.2150834.

Chakraborty, T., Das, K. and Kundu, P.K. (2018), "Framing the impact of external magnetic field on bioconvection of a nanofluid flow containing gyrotactic microorganisms with convective boundary conditions", *Alexandria Eng. J.*, **57**(1), 61-71. https://doi.org/10.1016/j.aej.2016.11.011.

Choi, S.U. and Eastman, J.A. (1995), Enhancing thermal conductivity of fluids with nanoparticles, (No. ANL/MSD/CP-84938; CONF-951135-29), Argonne National Lab., IL, U.S.A.

Ebrahimi, F., Dabbagh, A., Rabczuk, T. and Tornabene, F. (2019), "Analysis of propagation characteristics of elastic waves in heterogeneous nanobeams employing a new two-step porosity-dependent homogenization scheme", *Adv. Nano Res., Int. J.*, **7**(2), 135-143. https://doi.org/10.12989/anr.2019.7.2.135.

Eltaher, M.A., Almalki, T.A., Ahmed, K.I. and Almitani, K.H. (2019), "Characterization and behaviors of single walled carbon nanotube by equivalent-continuum mechanics approach", *Adv. Nano Res., Int. J.*, **7**(1), 39-49. https://doi.org/10.12989/anr.2019.7.1.039.

Ghalandari, M., Mirzadeh Koohshahi, E., Mohamadian, F., Shamshirband, S. and Chau, K.W. (2019), "Numerical simulation of nanofluid flow inside a root canal", *Eng. Applicat. Computat. Fluid Mech.*, **13**(1), 254-264. https://doi.org/10.1080/19942060.2019.1578696.

Gholinia, M., Hosseinzadeh, K., Mehrzadi, H., Ganji, D.D. and Ranjbar, A.A. (2019), "Investigation of MHD Eyring-Powell fluid flow over a rotating disk under effect of homogeneous-heterogeneous reactions", *Case Studies. Thermal Eng.*, **13**, 100356. https://doi.org/10.1016/j.csite.2018.11.007.

Guo, C., Hu, M., Li, Z., Duan, F., He, L., Zhang, Z., Marchetti, F., Du, M. (2020), "Structural hybridization of bimetallic zeolitic imidazolate framework (ZIF) nanosheets and carbon nanofibers for efficiently sensing α-synuclein oligomers", *Sensor. Actuat. B-Chem.*, **309**, 127821. https://doi.org/10.1016/j.snb.2020.127821.

Hafeez, A., Khan, M. and Ahmed, J. (2020), "Stagnation point flow of radiative Oldroyd-B nanofluid over a rotating disk", *Comput. Meth. Prog. Bio.*, **191**, 105342. https://doi.org/10.1016/j.cmpb.2020.105342.

Hu, Z., Lu, W. and Thouless, M.D. (2015), "Slip and wear at a corner with Coulomb friction and an interfacial strength", *Wear*, **338**, 242-251. https://doi.org/10.1016/j.wear.2015.06.010.

Hu, Z., Lu, W., Thouless, M.D. and Barber, J.R. (2016), "Effect of plastic deformation on the evolution of wear and local stress fields in fretting", *Int. J. Solids Struct.*, **82**, 1-8. https://doi.org/10.1016/j.ijsolstr.2015.12.031.

Huminic, G. and Huminic, A. (2020), "Entropy generation of nanofluid and hybrid nanofluid flow in thermal systems: A review", *J. Mol. Liq.*, **302**, 112533. https://doi.org/10.1016/j.molliq.2020.112533.

Khan, M.I., Hafeez, M.U., Hayat, T., Khan, M.I. and Alsaedi, A. (2020a), "Magneto rotating flow of hybrid nanofluid with entropy generation", *Comput. Meth. Prog. Bio.*, **183**, 105093. https://doi.org/10.1016/j.cmpb.2019.105093.

Khan, N.S., Shah, Q., Bhaumik, A., Kumam, P., Thounthong, P. and Amiri, I. (2020b), "Entropy generation in bioconvection nanofluid flow between two stretchable rotating disks", *Scientific Reports*, **10**(1), 1-26. https://doi.org/10.1038/s41598-020-61172-2.

Liu, C., Huang, X., Wu, Y.Y., Deng, X., Liu, J., Zheng, Z. and Hui, D. (2020), "Review on the research progress of cement-based and geopolymer materials modified by graphene and graphene oxide", *Nanotechnol. Rev.*, **9**(1), 155-169. https://doi.org/10.1515/ntrev-2020-0014.

Ma, Y., Mohebbi, R., Rashidi, M.M., Yang, Z. and Sheremet, M.A. (2019), "Numerical study of MHD nanofluid natural convection in a baffled U-shaped enclosure", *Int. J. Heat Mass Trans.*, **130**, 123-134. https://doi.org/10.1016/j.ijheatmasstransfer.2018.10.072.

Miklavčič, M. and Wang, C.Y. (2004), "The flow due to a rough rotating disk", *Zeitschrift für angewandte Mathematik und Physik ZAMP*, **55**(2), 235-246. https://doi.org/10.1007/s00033-003-2096-6.

Nasiri, H., Jamalabadi, M.Y.A., Sadeghi, R., Safaei, M.R., Nguyen, T.K and Shadloo, M.S. (2019), "A smoothed particle hydrodynamics approach for numerical simulation of nano-fluid flows", *J. Therm. Anal. Calorim.*, **135**(3), 1733-1741. https://doi.org/10.1007/s10973-018-7022-4.

Noghrehabadi, A., Behseresht, A. and Ghalambaz, M. (2013), "Natural convection of nanofluid over vertical plate embedded in porous medium: Prescribed surface heat flux", *Appl. Math. Mech.*, **34**(6), 669-686. https://doi.org/10.1007/s10483-013-1699-6.

Pedley, T.J., Hill, N.A. and Kessler, J.O. (1988), "The growth of bioconvection patterns in a uniform suspension of gyrotactic micro-organisms", *J. Fluid Mech.*, **195**, 223-237. http://doi.org/10.1017/S0022112088002393.

Rashidi, M.M., Abelman, S. and Mehr, N.F. (2013), "Entropy generation in steady MHD flow due to a rotating porous disk in a nanofluid", *Int. J. Heat Mass Trans.*, **62**, 515-525. https://doi.org/10.1016/j.ijheatmasstransfer.2013.03.004.

Safaei, B., Khoda, F.H. and Fattahi, A.M. (2019), "Non-classical plate model for single-layered graphene sheet for axial buckling", *Adv. Nano Res., Int. J.*, **7**(4), 265-275. https://doi.org/10.12989/anr.2019.7.4.265.

Saini, S. and Sharma, Y.D. (2018), "Analysis of onset of bio-thermal convection in a fluid containing gravitactic microorganisms by the energy method", *Chinese J. Phys.*, **56**(5), 2031-2038. https://doi.org/10.1016/j.cjph.2018.09.001.

Shah, Z., Dawar, A., Kumam, P., Khan, W. and Islam, S. (2019), "Impact of nonlinear thermal radiation on MHD nanofluid thin film flow over a horizontally rotating disk", *Appl. Sci.*, **9**(8), 1533. https://doi.org/10.3390/app9081533.

Shahsavari, D., Karami, B. and Janghorban, M. (2019), "Size-dependent vibration analysis of laminated composite plates", *Adv. Nano Res., Int. J.*, **7**(5), 337-349. https://doi.org/10.12989/anr.2019.7.5.337.

Sharma, K. and Gupta, S. (2017), "Viscous dissipation and thermal radiation effects in MHD flow of Jeffrey nanofluid through impermeable surface with heat generation/absorption", *Nonlinear Eng.*, **6**(2), 153-166.

Sheikholeslami, M. and Farshad, S.A. (2020), "Nanoparticle transportation inside a tube with quad-channel tapes involving solar radiation", *Powder Technol.*, **378**, 145-159. https://doi.org/10.1016/j.powtec.2020.09.041.

Sheikholeslami, M., Hatami, M. and Ganji, D.D. (2013), "Analytical investigation of MHD nanofluid flow in a semi-porous channel", *Powder Technol.*, **246**, 327-336. https://doi.org/10.1016/j.powtec.2013.05.030.

Sheikholeslami, M., Hatami, M. and Ganji, D.D. (2014), "Nanofluid flow and heat transfer in a rotating system in the presence of a magnetic field", *J. Mole. Liq.*, **190**, 112-120. https://doi.org/10.1016/j.molliq.2013.11.002.

Sheikholeslami, M., Farshad, S.A., Shafee, A. and Babazadeh, H. (2020a), "Performance of solar collector with turbulator involving nanomaterial turbulent regime", *Renew. Energ.*, **163**, 1222-1237. https://doi.org/10.1016/j.renene.2020.08.144.

Sheikholeslami, M., Jafaryar, M., Shafee, A. and Babazadeh, H.

(2020b), "Acceleration of discharge process of clean energy storage unit with insertion of porous foam considering nanoparticle enhanced paraffin", *J. Clean. Prod.*, **261**, 121206. https://doi.org/10.1016/j.jclepro.2020.121206

Subhani, M. and Nadeem, S. (2019), "Numerical analysis of micropolar hybrid nanofluid", *Appl. Nanosci.*, **9**(4), 447-459. https://doi.org/10.1007/s13204-018-0926-2.

Tlili, I., Bhatti, M.M., Hamad, S.M., Barzinjy, A.A., Sheikholeslami, M. and Shafee, A. (2019), "Macroscopic modeling for convection of Hybrid nanofluid with magnetic effects", *Physica A.*, **534**, 122136. https://doi.org/10.1016/j.physa.2019.122136.

Turkyilmazoglu, M. (2014), "Nanofluid flow and heat transfer due to a rotating disk", *Comput. Fluids*, **94**, 139-146. https://doi.org/10.1016/j.compfluid.2014.02.009.

Von Karman T. (1921) "Uberlaminare and turbulente Reibung", *ZAMM-J. Appl. Math. Mech.*, **1**(4), 233-252. https://doi.org/10.1007/s10973-020-09421-4.

Wang, H., Hu, Z., Lu, W. and Thouless, M.D. (2017), "The effect of coupled wear and creep during grid-to-rod fretting", *Nucl. Eng. Des.*, **318**, 163-173. https://doi.org/10.1016/j.nucengdes.2017.04.018.

Wang, G., Yao, Y., Chen, Z. and Hu, P. (2019), "Thermodynamic and optical analyses of a hybrid solar CPV/T system with high solar concentrating uniformity based on spectral beam splitting technology", *Energy*, **166**, 256-266. https://doi.org/10.1016/j.energy.2018.10.089.

Waqas, H., Khan, S.U., Hassan, M., Bhatti, M.M. and Imran, M. (2019), "Analysis on the bioconvection flow of modified second-grade nanofluid containing gyrotactic microorganisms and nanoparticles", *J. Mole. Liq.*, **291**, 111231. https://doi.org/10.1016/j.molliq.2019.111231.

Xun, S., Zhao, J., Zheng, L. and Zhang, X. (2017), "Bioconvection in rotating system immersed in nanofluid with temperature dependent viscosity and thermal conductivity", *Int. J. Heat Mass Trans.*, **111**, 1001-1006. https://doi.org/10.1016/j.ijheatmasstransfer.2017.04.074.

Yan, H., Xue, X., Chen, W., Wu, X., Dong, J., Liu, Y. and Wang, Z. (2020), "Reversible Na^+ insertion/extraction in conductive polypyrrole-decorated $NaTi_2(PO_4)_3$ nanocomposite with outstanding electrochemical property", *Appl. Surf. Sci.*, **530**, 147295. https://doi.org/10.1016/j.apsusc.2020.147295.

Yu, H., Dai, W., Qian, G., Gong, X., Zhou, D., Li, X. and Zhou, X. (2020), "The NO_x Degradation Performance of Nano-TiO_2 Coating for Asphalt Pavement", *Nanomaterials*, **10**(5), 897. https://doi.org/10.3390/nano10050897.

Zhao, G., Wang, Z. and Jian, Y. (2019), "Heat transfer of the MHD nanofluid in porous microtubes under the electrokinetic effects", *Int. J. Heat Mass Trans.*, **130**, 821-830. https://doi.org/10.1016/j.ijheatmasstransfer.2018.11.007.

Zhu, Z., Liu, Q., Liu, X. and Shui, J. (2020), "Temperature Impacts on Oxygen Reduction Reaction Measured by the Rotating Disk Electrode Technique", *J. Phys. Chem. C*, **124**(5), 3069-3079. https://doi.org/10.1021/acs.jpcc.9b10173.